Dopamine-modified α-synuclein blocks chaperone-mediated autophagy

Marta Martinez-Vicente,[1,2] Zsolt Talloczy,[3,4] Susmita Kaushik,[1,2] Ashish C. Massey,[1,2] Joseph Mazzulli,[5] Eugene V. Mosharov,[3,4] Roberto Hodara,[5] Ross Fredenburg,[6] Du-Chu Wu,[4,7] Antonia Follenzi,[2] William Dauer,[4] Serge Przedborski,[4,7] Harry Ischiropoulos,[5] Peter T. Lansbury,[6] David Sulzer,[3,4] and Ana Maria Cuervo[1,2]

[1]Department of Anatomy and Structural Biology and [2]Marion Bessin Liver Research Center, Albert Einstein College of Medicine of Yeshiva University, New York, New York, USA. [3]Department of Psychiatry, Department of Pharmacology, and [4]Department of Neurology, Columbia University, Department of Neuroscience, New York State Psychiatric Institute, New York, New York, USA. [5]Stokes Research Institute and Department of Pediatrics and Pharmacology, Children's Hospital of Philadelphia and the University of Pennsylvania, Philadelphia, Pennsylvania, USA. [6]Center for Neurologic Diseases, Brigham and Women's Hospital, Department of Neurology, Harvard Medical School, Cambridge, Massachusetts, USA. [7]Department of Pathology and Cell Biology, Columbia University, Department of Neuroscience, New York State Psychiatric Institute, New York, New York, USA.

Altered degradation of α-synuclein (α-syn) has been implicated in the pathogenesis of Parkinson disease (PD). We have shown that α-syn can be degraded via chaperone-mediated autophagy (CMA), a selective lysosomal mechanism for degradation of cytosolic proteins. Pathogenic mutants of α-syn block lysosomal translocation, impairing their own degradation along with that of other CMA substrates. While pathogenic α-syn mutations are rare, α-syn undergoes posttranslational modifications, which may underlie its accumulation in cytosolic aggregates in most forms of PD. Using mouse ventral medial neuron cultures, SH-SY5Y cells in culture, and isolated mouse lysosomes, we have found that most of these posttranslational modifications of α-syn impair degradation of this protein by CMA but do not affect degradation of other substrates. Dopamine-modified α-syn, however, is not only poorly degraded by CMA but also blocks degradation of other substrates by this pathway. As blockage of CMA increases cellular vulnerability to stressors, we propose that dopamine-induced autophagic inhibition could explain the selective degeneration of PD dopaminergic neurons.

Introduction

Parkinson disease (PD), the most common neurodegenerative movement disorder, is characterized by an extensive and progressive loss of neurons, most notably more than 80% of the dopaminergic neurons from the substantia nigra (SN) and the norepinephrinergic neurons of the locus coeruleus (LC), with less substantial death in several other brain regions. Accumulation of toxic forms of α-synuclein (α-syn) may be a critical step in the development of PD and other neurodegenerative proteinopathies, collectively referred to as synucleinopathies (1–4). α-Syn can adopt several conformational states (natively unfolded monomer, a β-sheet rich oligomer, protofibril, and a stable amyloid fibril) (1). Impaired degradation of α-syn in the affected neurons seems to underlie the accumulation of potentially toxic protofibrils and posttranslationally modified forms of α-syn that are thought to lead to formation of Lewy bodies, cytosolic inclusions that contain α-syn and are a pathological hallmark of the disease (5–8). Evidence supporting degradation of α-syn by both the ubiquitin/proteasome system and lysosomes (autophagy) has been presented (6, 7, 9). We reported lysosomal degradation of soluble wild-type α-syn via chaperone-mediated autophagy (CMA) (9). α-Syn is recognized first by a cytosolic chaperone and then binds to the lysosomal-associated membrane protein type 2A (LAMP-2A), a CMA receptor at the lysosomal membrane (10). Assisted by a luminal chaperone, α-syn crosses the lysosomal membrane and is rapidly degraded by proteases inside lysosomes (11). Two mutant forms of α-syn described in familial PD patients are poorly degraded via CMA (9) but bind to the CMA lysosomal receptor with higher affinity than any other known substrates, thus resulting in CMA blockage (9). Blockage of mutant α-syn degradation contributes to its increased cytosolic levels and may promote its aggregation. Aggregates of α-syn can also be degraded in lysosomes but via macroautophagy (6), a higher capacity autophagic pathway (12). Blockage of either CMA (13) or of the ubiquitin/proteasome system (14), both reported to occur in PD brains, induces macroautophagy, providing a possible explanation for the upregulation of this autophagic pathway in PD neurons.

In addition to the rare α-syn mutations, phosphorylated, ubiquitinated, nitrated and oxidized forms of α-syn have been identified in cytosolic aggregates in experimental models and brains from PD patients (1, 15–17). A modified form of α-syn suggested to be responsible for neuron toxicity results from a noncovalent interaction of α-syn and oxidized dopamine (18–20). Human SN and LC neurons produce dopaminochrome (oxidized dopamine), as this compound is the building block of neuromelanin, the pigment in SN and LC neurons (18, 21). Little is known, however, about the consequences of these modifications on α-syn turnover. On this basis, we asked whether these modifications affected the degradation of α-syn via CMA and analyzed the effect of these modified forms of α-syn on CMA activity. We report here that, although all modified forms of α-syn are less susceptible to CMA degradation, only dopamine-modified α-syn (DA–α-syn) interferes with CMA activity, providing a potential explanation for the preferential loss of SN and LC neurons in PD.

Nonstandard abbreviations used: CMA, chaperone-mediated autophagy; DA–α-syn, dopamine-modified α-syn; DAC–α-syn, dopaminochrome-modified α-syn; LAMP-2A, lysosomal-associated membrane protein type 2A; LC, locus coeruleus; MOPS, 3-(*N*-morpholino) propanesulfonic acid; PD, Parkinson disease; SN, substantia nigra; α-syn, α-synuclein; TH1, tyrosine hydroxylase–1; VM, ventral midbrain.

Conflict of interest: The authors have declared that no conflict of interest exists.

Citation for this article: *J. Clin. Invest.* **118**:777–788 (2008). doi:10.1172/JCI32806.

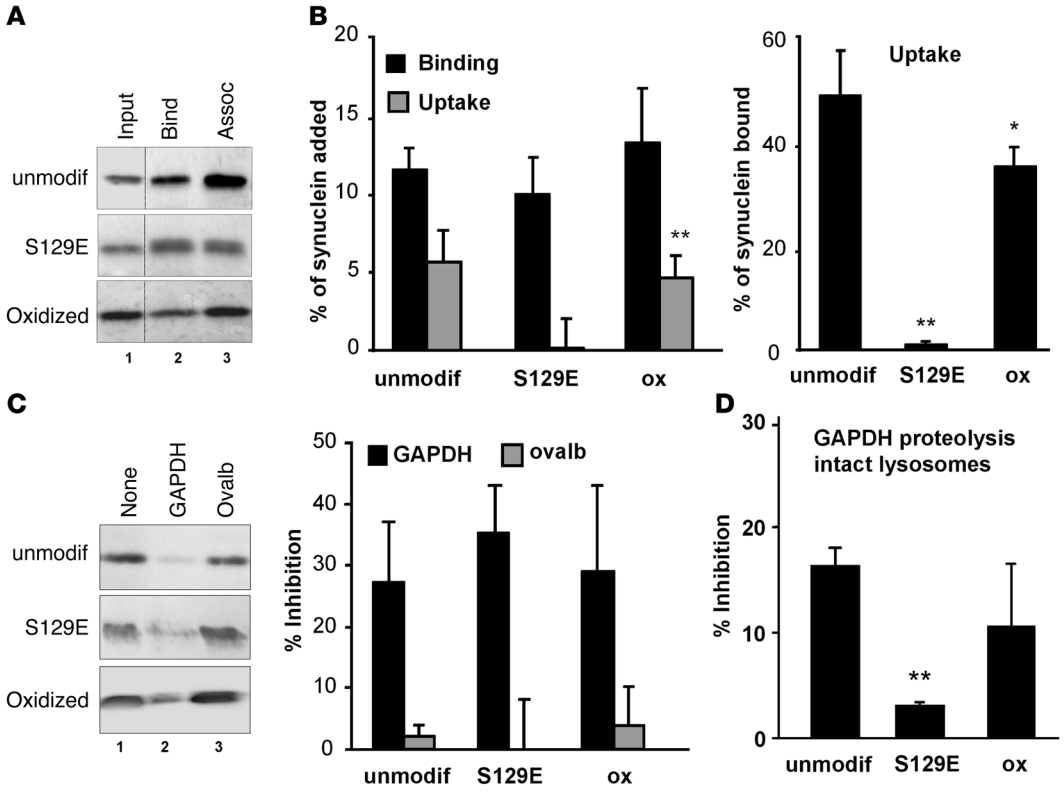

Figure 1
Effect of oxidation and phosphorylation of α-syn on its degradation in lysosomes by CMA. (**A**) Association of unmodified and oxidized α-syn and of the S129E mutant of α-syn with isolated lysosomes untreated (binding [Bind]) or previously treated with proteinase inhibitors (association: binding + uptake [Assoc]). Lane 1 shows one-tenth of the amount of protein added to the incubation (Input). (**B**) Percentage of each protein bound and translocated (uptake = association – binding) inside lysosomes calculated from the densitometric quantification of 11–13 immunoblots such as the representative immunoblots shown in **A**. The right-hand bars show the percentage of α-syn bound to the lysosomal membrane that was translocated into lysosomes. (**C**) Effect of a 2-molar excess of GAPDH or ovalbumin (Ovalb) on the association of unmodified, oxidized, and S129E mutant α-syn with lysosomes. Left panel: representative immunoblot. Right panel: percentage of inhibition of the lysosomal association of each form of α-syn calculated from the densitometric quantification of 4–6 immunoblots such as those shown here. (**D**) Effect of adding these 3 forms of α-syn in equimolar ratio with [^{14}C]GAPDH on the degradation of [^{14}C]GAPDH by intact lysosomes. Values are expressed as percentage of inhibition of GAPDH degradation and are mean + SEM of 4–5 experiments with triplicate samples. *P < 0.05; **P < 0.01.

Results

Phosphorylation alters CMA of α-syn. Since phosphorylated and oxidized forms of α-syn each accumulate in inclusion bodies upon treatment of cultured cells with oxidants (15, 16), we analyzed the effects of these 2 modifications on CMA of α-syn. Phosphorylation was emulated by replacing serine 129 with the negatively charged residue glutamic acid (S129E) (pseudophosphorylation). This modification has been shown to mimic the biochemical and biophysical properties of the α-syn phosphorylation described in brain tissues from PD patients (16). Using amino acid replacement rather than in vitro phosphorylation ensured that the protein remained "phosphorylated-like" after exposure to the lysosomal fraction, which is highly enriched in phosphatases. We induced different degrees of α-syn oxidation by incubation of the purified protein with a pro-oxidizing solution for increasing periods of time. We selected conditions resulting in the highest level of oxidation (measured by the content of carbonyl groups) for which the protein remained soluble (exposure to the pro-oxidizing solution for more than 90 minutes resulted in α-syn aggregation). None of these modifications interfered with the ability of the antibody against α-syn to recognize these proteins (determined by comparing Coomassie blue staining and immunoblot of the purified proteins subjected to SDS-PAGE; data not shown).

The most direct test of whether a protein is a CMA substrate is to measure its binding, uptake, and degradation in isolated lysosomes (22–24). In this in vitro system, binding and uptake of substrate proteins can be separately calculated (25). We first verified that the integrity of the lysosomes was not altered by modified forms of α-syn and that, once translocated into the lysosomal lumen, the proteins were rapidly degraded. In contrast to the destabilizing effect of modified forms of α-syn on chromaffin-dense core vesicles (26), concentrations up to 17 μM of any of the forms of α-syn used in this study did not significantly alter the stability of the membrane of CMA-active rat liver lysosomes (Supplemental Figure 1; supplemental material available online with this article; doi:10.1172/JCI32806DS1). None of the forms of α-syn displayed resistance to degradation by lysosomal matrix extracts (Supplemental Figure 2).

Wild-type α-syn, oxidized α-syn, and the S129E mutant α-syn exhibited similar lysosomal-binding abilities, but the phosphorylation-like mutant did not translocate across the lysosomal

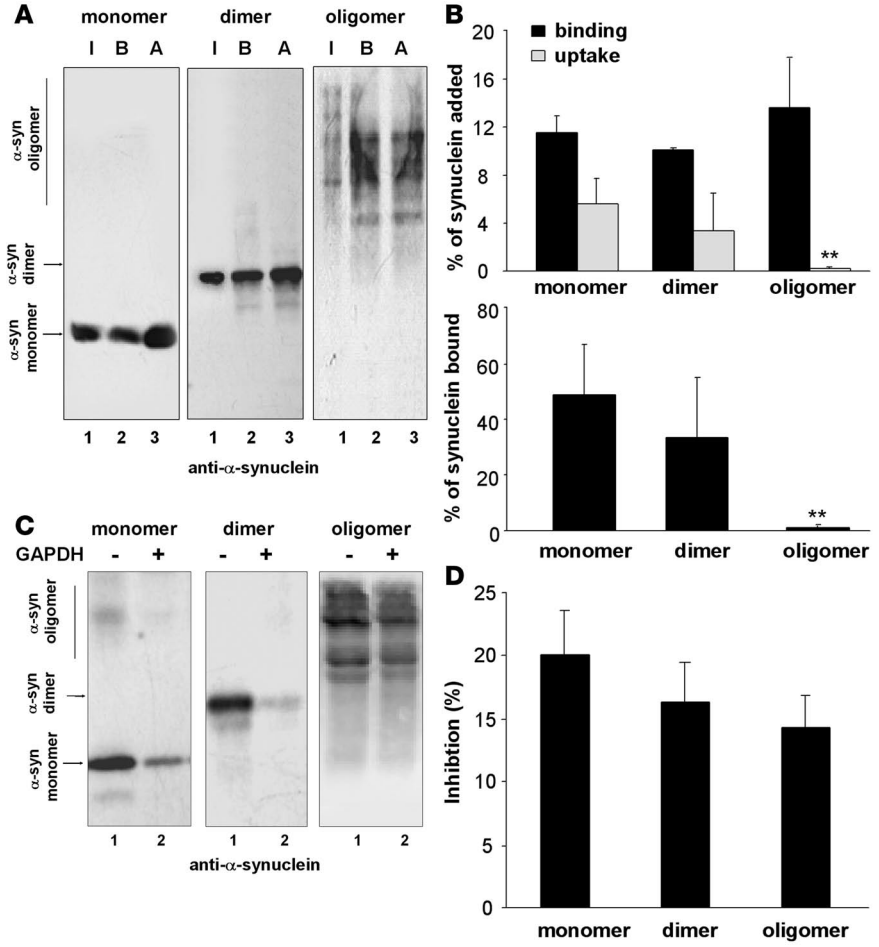

Figure 2

Degradation in lysosomes by CMA of multimeric forms of α-syn. (**A**) Association of monomers and irreversibly cross-linked dimers and oligomers of α-syn with isolated lysosomes untreated (binding [B]) or previously treated with proteinase inhibitors (association [A]). Lane 1 shows one-tenth of the amount of protein added to the incubation (input [I]). (**B**) Upper panel: percentage of each protein bound and translocated (uptake = association – binding) inside lysosomes, calculated from the densitometric quantification of 6–8 immunoblots as used for the immunoblots shown in **A**. Lower panel: percentage of α-syn bound to the lysosomal membrane that is translocated into lysosomes. (**C**) Effect of a 2-molar excess of GAPDH on the association of monomeric, dimeric, or multimeric α-syn with lysosomes. (**D**) Percentage of inhibition of the lysosomal association of each form of α-syn calculated from the densitometric quantification of 4–6 immunoblots such as those shown in **C**. $^{**}P < 0.01$.

membrane (addition of protease inhibitors did not increase the amount of S129E α-syn associated with lysosomes) (Figure 1, A and B), even after normalization for the amount of protein bound to lysosomes (Figure 1B). A considerable decrease in α-syn uptake was also observed when we used an in vitro phosphorylated form of the protein (Supplemental Figure 3). However, due to the higher variability among samples, attributable to partial dephosphorylation of the protein during incubation, we used the pseudophosphorylated mutant protein for quantitative analysis and competition assays. Binding of S129E mutant still occurred at the CMA receptor, as the bound protein can be displaced by the well-characterized CMA substrate GAPDH but not by ovalbumin, a non-CMA substrate (Figure 1C). The S129E mutant did not compete as effectively for CMA of GAPDH (measured here as its degradation by intact lysosomes, which recapitulates binding, uptake, and proteolysis) as unmodified or oxidized wild-type α-syn (Figure 1D). These results suggest that the S129E α-syn binds with comparatively low affinity to the CMA receptor at the lysosomal membrane and consequently does not interfere with the lysosomal internalization of other substrates by this pathway. Oxidation of α-syn moderately reduced its efficiency of lysosomal translocation (Figure 1, A and B) but similarly did not interfere with CMA function. Lysosomal-bound oxidized α-syn can be displaced by GAPDH, and it displays only a slightly lower ability than unmodified α-syn to compete with CMA of GAPDH (Figure 1, C and D).

Oligomeric forms of α-syn cannot be taken up by lysosomes via CMA. α-Syn can exist in a variety of multimeric states (1), and covalent modifications of the protein promote its oligomerization (15, 18, 27). Exposure to nitrating agents results in tyrosine nitration of monomeric α-syn and formation of both nitrated and nonnitrated dimers and oligomers (28). Because substrate unfolding is required for CMA (25), large aggregates cannot be degraded by this pathway, but CMA of smaller α-syn oligomers has not been previously evaluated. We isolated multimeric forms produced by exposure of α-syn to nitrating agents (27) and compared their degradation by CMA. We tracked CMA of these fractions separately with antibodies that recognize either α-syn (Figure 2) or the tyrosine-nitrated epitopes in α-syn (Figure 3) (27). Monomer, dimer, and oligomer forms of α-syn bound to the lysosomal membrane, but only monomers and dimers were translocated (Figure 2, A and B). Interestingly, the covalently cross-linked dimers of α-syn did not require disassembly before translocation, as they were detected as dimers in the lysosomal lumen. Nitration slightly decreased both binding and uptake of monomers and dimers (Figure 3, A and B) but not their ability to inhibit CMA of GAPDH (Figure 3D). As observed for the unmodified oligomers, nitrated oligomeric α-syn did not translocate into lysosomes (Figure 3, A and B). Binding of the nitrated oligomers to the lysosomal membrane was poorly blocked by GAPDH (Figure 3C), in contrast to the binding of nonnitrated α-syn (Figure 2, C and D) and other α-syn forms (Figure 3C). Unfortunately, aggregation of oligomers of α-syn under the

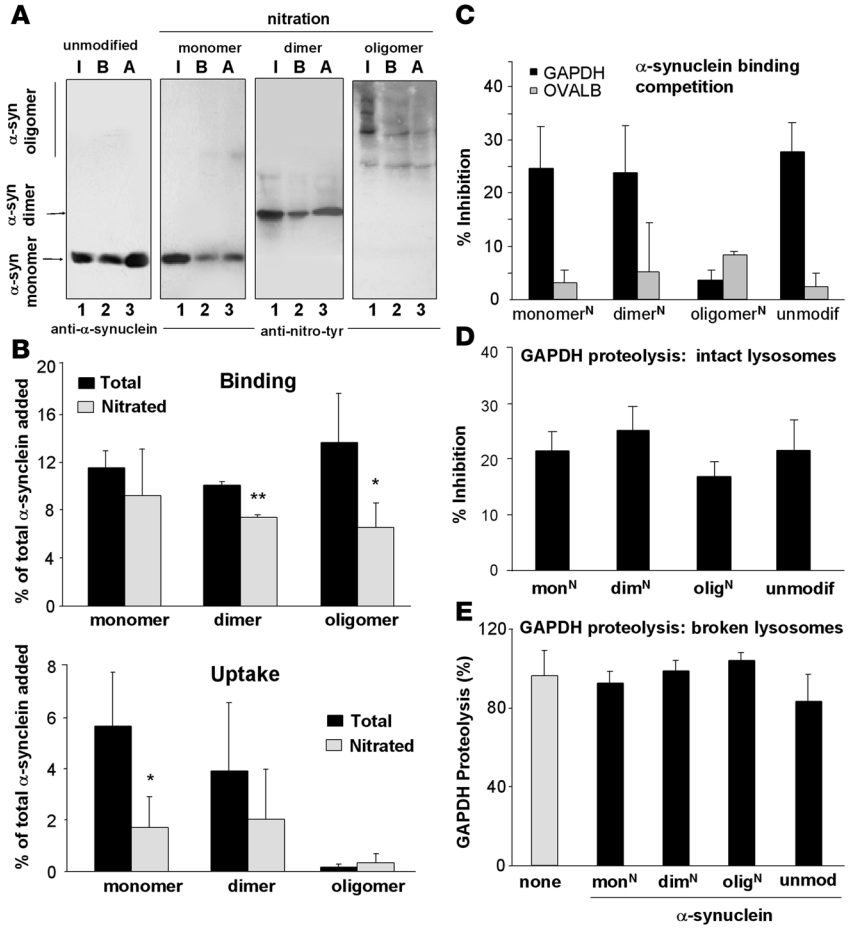

Figure 3

Effect of nitration of α-syn on its degradation in lysosomes by CMA. (**A**) Association of unmodified α-syn and the monomeric, dimeric, and oligomeric forms resulting from nitration of α-syn with isolated lysosomes untreated (binding [B]) or previously treated with proteinase inhibitors (association: binding + uptake [A]). Input (I): one-fifth of the amount of protein added to the incubation. Blots were developed with an antibody against α-syn (unmodified protein) or one that only recognizes the nitrated forms of α-syn (nitrated samples). (**B**) Percentage of each protein bound (upper panel) and translocated (lower panel) inside lysosomes, calculated from the densitometric quantification of immunoblots developed with both antibodies. $n = 6$. (**C**) Effect of a 2-molar excess of GAPDH on the association of monomers, dimers, and oligomers of nitrated α-syn (N) with lysosomes. Values are expressed as percentage of inhibition of the lysosomal association of each form of α-syn. $n = 4–6$. (**D** and **E**) Effect of equimolar amounts of unmodified monomers (unmodif) and nitrated (N) monomers (mon), dimers (dim), and oligomers (olig) of α-syn on the degradation of [^{14}C]GAPDH by intact (**D**) or broken (**E**) lysosomes. Values are expressed as percentage of inhibition of the degradation of GAPDH (**D**) or as percentage of GAPDH degradation at the end of incubation (**E**) and are mean + SEM of 4–5 experiments with triplicate samples. *$P < 0.05$; **$P < 0.01$.

conditions required for coimmunoprecipitation of CMA substrates with the lysosomal receptor prevented us from conclusively documenting the absence of binding of nitrated oligomers directly to the CMA receptor. In conclusion, while oligomerization and nitration of α-syn reduced its clearance through CMA, none of these forms affected lysosomal CMA activity.

DA–α-syn blocks CMA. Finally, we analyzed DA–α-syn as a CMA substrate. We exposed α-syn to dopamine (DA–α-syn) or its autooxidized product, dopaminochrome (DAC–α-syn) (18). DA– and DAC–α-syn were poorly translocated inside lysosomes, even though their binding was significantly higher than that of unmodified α-syn (Figure 4A). GAPDH did not inhibit the binding of DA– and DAC–α-syn to lysosomes (Figure 4B), but both modified forms of α-syn showed a significantly higher inhibitory effect on CMA of GAPDH (2.8-fold higher inhibition than observed for the wild-type protein) (Figure 4C). Considering the short duration of our transport assay (30 minutes), we hypothesize that this inhibitory effect should have severe consequences on CMA in the cellular context, where CMA activation persists for longer periods of time. Remarkably, the effects of DA– and DAC–α-syn closely resembled those of the pathogenic PD mutants of α-syn that cause familial PD, as they (a) bind tightly to the lysosomal membrane; (b) translocate poorly into lysosomes; and (c) block the lysosomal uptake of CMA substrates (9). The effect of dopamine on α-syn was independent of protein oxidation and specific for dopamine-induced conformational changes on the protein because equivalent treatment of a mutant form of α-syn (mutant α-syn, in which the residues $Y_{125}EMPS_{129}$ have been replaced by $F_{125}AAFA_{129}$, respectively) that is insensitive to dopamine-induced changes (18) did not modify its lysosomal binding or uptake (Supplemental Figure 3).

To further verify that the effect on CMA observed in vitro also occurs in neurons and is directly related to dopamine modification of α-syn, we determined whether the reaction of intracellular dopamine with α-syn would block CMA in SN neurons. To elevate cytosolic DA, we exposed postnatally derived mouse ventral midbrain (VM) cultures that encompass the SN and contain approximately 40% dopaminergic and 60% GABAergic (transmitting or secreting GABA) neurons (29) to the dopamine precursor L-DOPA. We have previously shown that this treatment augments the packing of catecholamines into individual vesicles and also increases total intracellular and cytosolic dopamine to a degree similar to that observed during α-syn overexpression (30, 31). As there is no method to measure cytosolic DA–α-syn formed within the cultures, we designed conditions to favor formation of cytosolic DA–α-syn to test whether this might interfere with CMA activity in neurons. Using a recently developed technique, intracellular patch electrochemistry (32), we measured neuronal cytosolic dopamine concentration in cultures derived from mice expressing green fluorescent protein behind a tyrosine hydroxylase promoter that allowed us to differentiate between dopaminergic and GABAergic cells. Both neuronal populations had native cytosolic dopamine levels beneath the detection limit of the technique

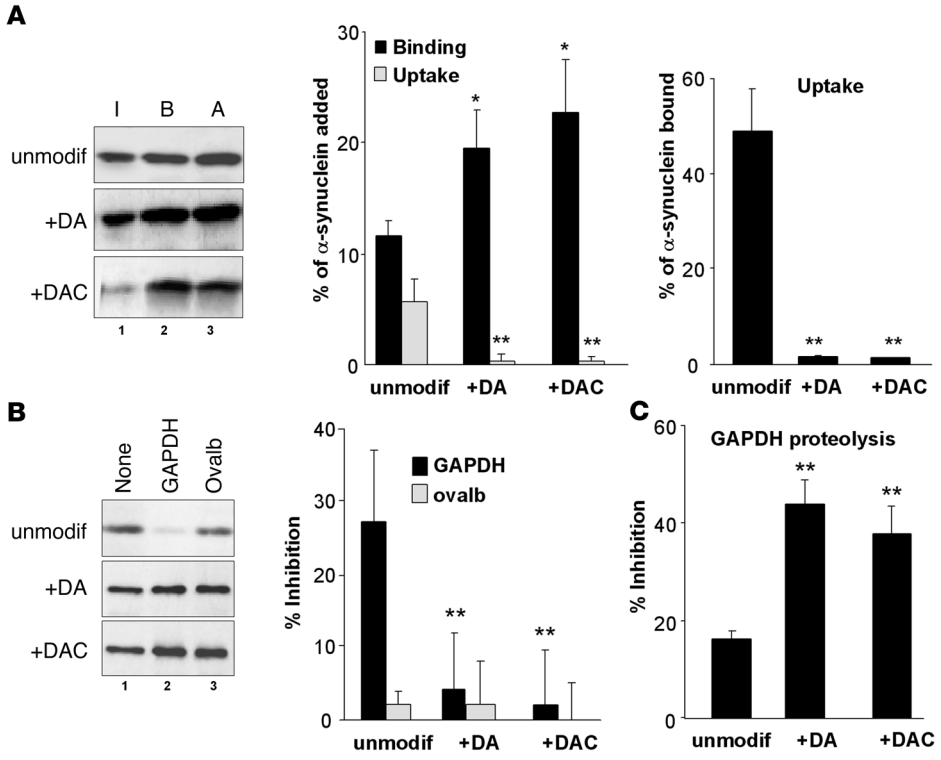

Figure 4

Degradation of dopamine-reacted α-syn in lysosomes by CMA. (**A**) Association of unmodified, dopamine-reacted (+DA) and dopaminochrome-reacted (+DAC) α-syn with isolated lysosomes untreated (binding [B]) or previously treated with proteinase inhibitors (association: binding + uptake [A]). Input (I): one-fifth of the amount of protein added to the incubation. The percentage of each protein bound and translocated inside lysosomes (middle) and the percentage of bound protein translocated into lysosomes (right) was calculated from the densitometric quantification of immunoblots. $n = 6–8$. (**B**) Effect of a 2-molar excess of GAPDH or ovalbumin (ovalb) on the association of unmodified and DA– and DAC–α-syn with lysosomes. Values are the percentage of inhibition of the lysosomal association of each form of α-syn. $n = 6$. (**C**) Effect of unmodified and DA– and DAC–α-syn in 0.5:1 molar ratio with [^{14}C]GAPDH in the degradation of [^{14}C]GAPDH by intact lysosomes. Values are mean + SEM of the percentage of GAPDH degradation at the end of the incubation in 4–5 experiments with triplicate samples. $^{**}P < 0.01$.

(<100 nM). Exposure to L-DOPA at 100 μM, a level that produces cytosolic dopaminochrome and neuromelanin (33) and eventually kills dopaminergic neurons but not the GABAergic neurons (34), increased cytosolic dopamine in unlabeled, predominantly GABAergic neurons to 2.5 ± 0.6 μM ($n = 20$), while in dopaminergic neurons, free cytosolic dopamine reached 17.7 ± 2.7 μM ($n = 34$, $P < 0.001$); thus, the level of dopamine reached in the neuronal cytosol was nearly identical to the dopamine concentration used to produce the DA–α-syn in vitro (14 μM).

L-DOPA exposure inhibited CMA activity (proteolysis sensitive to ammonium chloride but insensitive to the macroautophagy inhibitor, 3-methyladenine) in VM cultures by 48% (Figure 5A; rates of protein degradation by CMA changed from 0.52% ± 0.01% protein degraded/h to 0.27% ± 0.03% protein degraded/h), an impressive effect, considering that only approximately 40% of the neurons in these cultures are dopaminergic. In agreement with previous results (13), CMA inhibition enhanced macroautophagy (rates of protein degradation by macroautophagy changed from 0.20% ± 0.03% protein degraded/h to 0.38% ± 0.04% protein degraded/h). L-DOPA's inhibition of CMA was dependent on α-syn, as the pronounced inhibition of CMA activity was not observed in VM cultures derived from α-syn–null (–/–) mice (Figure 5A) (rates of degradation by CMA were 0.69% ± 0.06% and 0.54% ± 0.02% protein degraded/h in untreated and dopamine-treated cells, respectively) (35). In contrast to the effects of L-DOPA in VM cultures, L-DOPA had no effect on autophagy in cultures of cortical neurons (Figure 5B) (rates of degradation by CMA were 0.14% ± 0.03% and 0.21% ± 0.05% protein degraded/h in untreated and dopamine-treated cells respectively). Therefore, these results confirm that the inhibitory effect of DA–α-syn on CMA activity observed in the in vitro system occurs in neurons and prove that the combination of high (>3 μM) cytosolic dopamine and the presence of cytosolic α-syn was required for CMA inhibition. In support of the contribution of CMA blockage by α-syn to neurotoxicity, we found that treatment of L-DOPA in VM neuronal cultures in which CMA activity had been blocked by RNAi against LAMP-2A did not decrease cell viability (calculated as cellular loss) beyond the decrease already observed with the CMA blockage (Supplemental Figure 5). Blockage of CMA in the neuronal cultures resulted in considerable cellular loss, even in the absence of any treatment. However, in contrast to the neurotoxic effect of L-DOPA treatment in control cells, this treatment did not have a significant additive effect on the toxicity observed in the CMA-impaired cells (12% cell loss in CMA-impaired cells compared with 68% cell loss in control cells) (Supplemental Figure 5).

In order to further characterize the effect of DA–α-syn in lysosomes in intact cells, we used a cellular model system in which we could modulate the intracellular levels of dopamine by expression of the R37E/R38E (RR-EE) mutant form of human tyrosine hydroxylase–1 (TH1) and in which lysosomal isolation is feasible. In brief, we expressed a mutant TH1 that lacks dopamine feedback inhibition in retinoic acid–differentiated SH-SY5Y cells stably expressing wild-type α-syn or the dopamine-insensitive mutant α-syn (18).We have previously shown that expression of this mutant TH1 increased the intracellular steady state levels of dopamine (36), which inhibited the formation of α-syn aggregates and induced the formation of oligomeric intermediates (36). As in those previous studies, we optimized mutant TH1 expression to increase intracellular steady state levels of dopamine close to 100 femtomoles/μg of protein (36). We did not find significant changes in the overall contribution of autophagic pro-

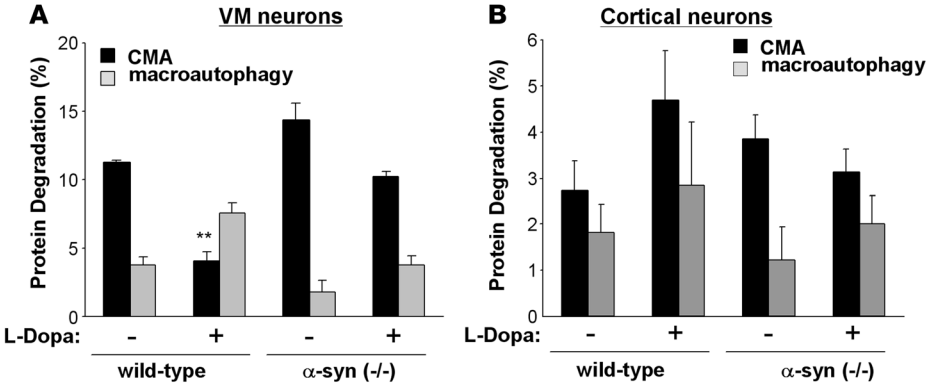

Figure 5

Dopamine-induced blockage of CMA in VM neuron cultures. Effect of L-DOPA treatment on the degradation rates of long-lived proteins in cultured dopaminergic neurons (VM neurons) (**A**) and cortical neurons (**B**) from wild-type and homozygous (–/–) α-syn–knockout mice. Protein degradation was calculated as the percentage of total protein (acid precipitable radioactivity) at time 0, converted into amino acids and small peptides (acid soluble radioactivity) after 20 hours. The contribution of different autophagies to total protein degradation was calculated as protein degradation sensitive to ammonium chloride and 3-methyladenine (macroautophagy) and protein degradation sensitive to ammonium chloride but insensitive to 3-methyladenine (CMA). $n = 3$ experiments with at least 6 dishes for each condition. $^{**}P < 0.01$.

tein degradation in any of the analyzed conditions (Figure 6A). However, increased steady state dopamine inhibited the proportion of autophagy due to CMA activity (proteolysis sensitive to ammonium chloride but insensitive to the macroautophagy inhibitor 3-methyladenine) by 52% in cells expressing wild-type α-syn but had no effect on cells expressing mutant α-syn (Figure 6B) (rates of protein degradation by CMA changed from 0.77% ± 0.08% to 0.34% ± 0.12% protein degraded/h after TH treatment in cells expressing wild-type α-syn). Likewise, only the lysosomes from cells expressing mutant TH1 and wild-type α-syn showed reduced rates of GAPDH degradation by CMA (Figure 6B).

Finally, to determine whether the dopamine-mediated inhibition of CMA was related to the association of the modified α-syn to the lysosomal membrane, we measured intracellular α-syn associated with the isolated lysosomes. We used standardized procedures for the isolation of a fraction highly enriched in lysosomes (less than 0.1% of contamination by nonlysosome-related structures) in which approximately 60% of lysosomes were active for CMA (contained heat shock cognate protein 70 [hsc70] in their lumen) (13, 37, 38). Most of the lysosome-associated protein (95%) under these conditions was bound to the cytosolic side of the lysosomal membrane, as the internalized protein was rapidly degraded during isolation. Immunoblot (Figure 6C) and immunogold (Figure 6D) analysis with an antibody specific against α-syn (39) revealed a 30% increase in the amount of monomeric α-syn associated with lysosomes from cells coexpressing mutant TH1 and wild-type α-syn (Figure 6, C and D), while the amount of mutant α-syn associated with lysosomes decreased under the same conditions (Figure 6C). The higher density of α-syn in particular areas of the lysosomal membrane detected as clusters of gold particles (>5 gold particles) by immunogold in cells coexpressing mutant TH1 and wild-type α-syn (Figure 6D) suggested some level of organization of this protein in the membrane. Using immunoblot procedures, we confirmed that, indeed, the combination of high intracellular dopamine and wild-type α-syn produced oligomers on the lysosomal surface (detected as higher molecular weight forms of α-syn in the immunoblot; Figure 6E). The oligomers did not appear to form larger aggregates (i.e., protofibrils and fibrils), as the α-syn signal was never detected in the interface between the running/stacking gel, in the wells when whole gels were subjected to immunoblot, or in the filter after subjecting the lysosomes to filter-retardation assays (data not shown). Oligomers were not observed in lysosomes isolated from cells expressing the dopamine-insensitive mutant α-syn (Figure 6E). These results confirm that an interaction between intracellular dopamine and α-syn enhances its binding to the lysosomal surface but blocks its translocation and that of other substrates into lysosomes via CMA.

To determine whether the oligomers of DA–α-syn bind with higher affinity to the lysosomal membrane than native α-syn or whether they form after the protein binds to the membrane, we incubated isolated lysosomes with unmodified α-syn or DA–α-syn and compared binding of monomers, dimers, and oligomers. As shown in Figure 7A, multimeric forms of α-syn were barely detectable in the preparation of unmodified protein and at the lysosomal membrane. However, more than 70% of the lysosome-associated DA–α-syn was in the form of dimers and oligomers (22% and 55%, respectively). Although dimers and oligomers of α-syn were also detectable in the purified DA–α-syn, they contributed less than 35% to the total α-syn in the fraction. These results indicate that binding of DA–α-syn to lysosomal membranes promotes its organization as oligomers. Likewise, immunogold analysis of lysosomes incubated with unmodified α-syn or DA–α-syn revealed that more than 60% of the lysosome-associated DA–α-syn was clustered (>5 gold particles) at the lysosomal membrane (Figure 7, B and C). The occasional clustering observed for the unmodified protein (which was less frequent and contained lower numbers of gold particles than for DA–α-syn) could be the result of saturation by the high concentrations of the protein presented to lysosomes. Consequently, the organization of DA–α-syn into oligomeric complexes at the lysosomal membrane seems to be responsible for the blockage of the CMA lysosomal translocation complex.

Discussion

In this study, we demonstrate that various posttranslational modifications of α-syn have different consequences for the ability of the protein to be degraded via CMA and different effects on CMA of other substrates. Only α-syn monomers and dimers, but not oligomers, are degraded via CMA. Oxidation and nitration of α-syn slightly inhibit degradation by CMA, while phosphorylation and exposure to dopamine almost completely prevent protein removal through this pathway. Notably, only DA–α-syn inhibited CMA activity in isolated lysosomes, cultured dopaminergic cell lines, and VM neurons.

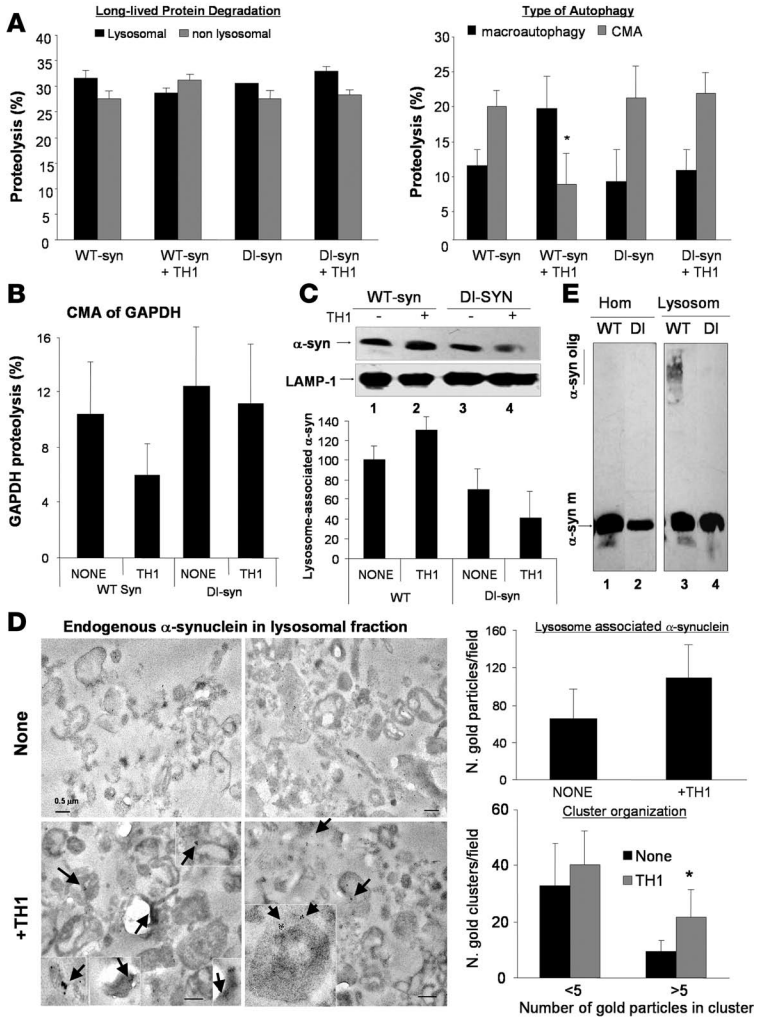

Figure 6

Increased intracellular levels of dopamine enhance the association of modified α-syn to lysosomes and block CMA. SH-SY5Y cells stably expressing wild-type (WT-syn) or a dopamine-insensitive mutant form of α-syn (DI–α-syn) were infected with an empty plasmid (none) or a plasmid encoding for mutant human TH1. (**A**) Protein degradation sensitive (lysosomal) or insensitive (nonlysosomal) to ammonium chloride (left) and protein degradation sensitive (macroautophagy) or insensitive (CMA) to 3-methyladenine. (**B**) Degradation via CMA of GAPDH by intact lysosomes isolated from the 4 different groups of cells. (**C**) Association of endogenous monomeric α-syn to lysosomes isolated from the same cells. Upper panel: representative immunoblot for α-syn and LAMP-1; lower panel: densitometric quantification of the amount of lysosome-associated α-syn (corrected per amount of lysosomes). (**D**) Left panels: Immunogold for α-syn of lysosomes isolated from cells stably expressing wild-type α-syn and an empty vector (none: upper panel) or a vector coding for TH1 (+TH: lower panel). The contribution of nonlysosomal structures to this fraction was less than 0.1%, and the percentage of total lysosomes active for CMA was 65%. Arrows: clusters (>5 particles) of gold particles. Insets: cluster-containing individual lysosomes at higher magnification. Scale bars: 0.5 μm. Right panels: number of gold particles associated with lysosomes per field (upper panel) and number of lysosome-associated clusters of more or less than 5 gold particles per field (lower panel) quantified in 4 different fields (≥50 lysosomes/field). (**E**) Presence of monomeric (α-syn m) and oligomeric (α-syn olig) forms of α-syn in total cellular homogenate (Hom) and in lysosomes (Lysosom) isolated from cells stably expressing wild-type or dopamine-insensitive mutant (DI–α-syn) and mutant TH1. All values are mean + SEM of cells cultured in 3 separate dishes or of triplicate samples. *$P < 0.05$.

There are a wide range of effects on CMA of α-syn depending on the type of protein modification. Although the reasons for their altered CMA remain elusive, it is possible that a low binding affinity of the native protein or a particular conformational change induced by its phosphorylation could be responsible for the poor lysosomal translocation of phosphorylated α-syn. Extensive oxidation of CMA substrates has been previously found to interfere with their translocation across the lysosomal membrane, likely as the result of aggregation once in the lipid environment of the membrane (40). A combination of the lipid-induced conformational changes described for α-syn (41) and those induced by the particular modifications could inhibit CMA of oxidized or nitrated α-syn. The failure of lysosomes to take up oligomeric α-syn could be in part due to an inability to disassemble into simpler α-syn forms compatible with membrane translocation or because the oligomers bind to the lysosomal membrane through CMA-independent mechanisms. In support of the latter hypothesis, membrane-bound nitrated oligomers could not be degraded by CMA or displaced by other CMA substrates but did not inhibit CMA more than the other forms. Unfortunately, aggregation of oligomers of α-syn under the conditions required for coimmunoprecipitation of CMA substrates with the lysosomal receptor prevented us from conclusively documenting the absence of binding of nitrated oligomers directly to the CMA receptor.

The inhibitory effect of DA–α-syn on CMA resembled that previously described for 2 of the mutations of α-syn identified in familial forms of PD (9). High intracellular levels of wild-type α-syn also inhibit CMA, although to a lesser extent (ref. 9 and A.M. Cuervo, L. Stefanis, and D. Sulzer, unpublished results). Because α-syn is one of the most efficient CMA substrates identified to date, it is possible that high cytosolic levels of the protein could saturate CMA for other substrates. However, we cannot discard the possibility that increased absolute content of α-syn would also increase the size of the pool of the protein undergoing posttranslational modifications. These modified forms of α-syn, and in particular that mediated by dopamine, could be directly responsible for the inhibitory effect on CMA observed under these conditions.

Although most of the modifications of α-syn impair its own CMA degradation, intracellular DA–α-syn could be particularly detrimental for the cells due to its additional inhibitory effect on CMA of other substrates. We have recently shown that cells respond to blockage of CMA by upregulating macroautophagy (13). This compensatory mechanism is sufficient to maintain normal rates of protein degradation to guarantee cell survival. Consistent with these previous findings, we found that blockage of CMA in SH-SY5Y cells with increased intracellular dopamine (Figure 6) and in VM cultures after exposure to L-DOPA resulting

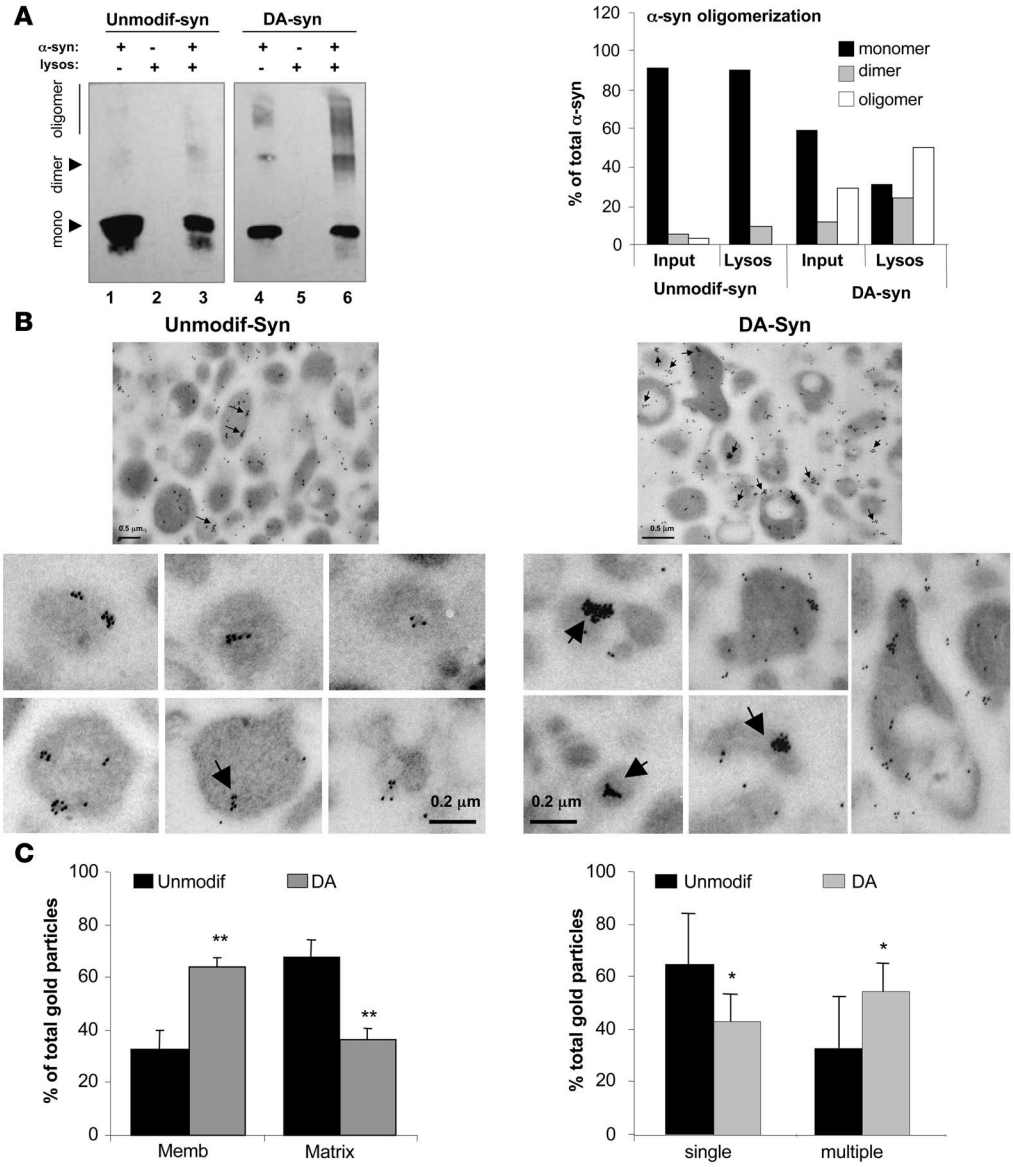

Figure 7

Organization of dopamine-reacted α-syn at the lysosomal membrane. (**A**) Association of unmodified (Unmodif-syn) and dopamine-reacted α-syn (DA-syn) to isolated lysosomes was analyzed after incubation by SDS-PAGE and immunoblot for α-syn. Monomers (mono), dimers, and oligomers are indicated by arrows. Lanes 1 and 4: one-tenth of the protein added to the incubation (inputs); lanes 2 and 5: lysosomes incubated alone; lanes 3 and 6: lysosomes incubated with α-syn. Right panel: percentage of α-syn in each of the different multimeric states in the input and associated with lysosomes was calculated by densitometric analysis of the immunoblots. (**B**) Electron microscopy and immunogold with an antibody against α-syn of lysosomes incubated as in **A**. The contribution of nonlysosomal structures to this fraction was less than 0.01%, and the percentage of total lysosomes active for CMA in this fraction was 95%. Arrows indicate clusters (>5) of gold particles. Panels on the bottom show individual lysosomes at higher magnification to better show the size of the gold particle clusters. (**C**) Percentage of gold particles associated with the lysosomal membrane and matrix (left panel) and present as single particles or organized in clusters (>5 gold particles) (right panel) in lysosomes incubated with unmodified and dopamine-reacted α-syn. Values are mean + SEM of the quantification of 4 fields (approximately 150 lysosomes). $^{*}P < 0.05$; $^{**}P < 0.01$.

in increased cytosolic DA (Figure 5) did not result in significant quantitative changes in the total degradation rates of long-lived proteins in lysosomes (as determined by sensitivity to ammonium chloride) due to compensatory macroautophagy. The observation that L-DOPA had much less effect on CMA in VM cultures from α-syn–null mice strongly suggests that a reaction between dopamine and α-syn is responsible for CMA blockage. The upregulation of macroautophagy observed in the VM cultures from α-syn–null mice treated with L-DOPA could be at least in part in response to intracellular protein aggregation (14, 42) or in part due to the remaining slight reduction in CMA, but in any case, the enhancement in macroautophagy in the cultures from α-syn–null mice is clearly lower than that observed in the wild-type VM neurons. Macroautophagy cannot, however, replace CMA under stress

conditions, as CMA blockage increases cellular vulnerability to stressors, resulting in apoptosis and cell death (13). The unique effect of DA–α-syn on CMA could be a cause of the massive loss of dopaminergic SN neurons in PD as well as norepinephrine-releasing neurons of the LC, which likewise possess cytosolic dopamine and produce neuromelanin, a product of dopamine modifications localized within macroautophagic organelles (33).

While a variety of modifications of α-syn likely occurred following treatment of cell lines and neurons with L-DOPA, the observations that CMA inhibition was more pronounced in dopaminergic neurons than in cortical neurons (Figure 5B) and that a dopamine-insensitive mutant of α-syn (still susceptible to oxidation) was efficiently degraded by CMA (Supplemental Figure 4) and did not interfere with CMA (Figure 6, A and B) further support a critical role for dopamine-mediated modifications of α-syn in the impaired CMA activity. The inhibitory effect of DA–α-syn on CMA did not result from a direct effect of dopamine on lysosomes because it was not observed when GAPDH was incubated with lysosomes with dopamine but in the absence of α-syn (data not shown). In addition, the effect observed for DA–α-syn could be reproduced with α-syn treated with the fully oxidized dopamine product (dopaminochrome), which indicates that the effect is not due to the oxidation of the protein or due to the oxidants generated during the oxidation of dopamine during the incubation with lysosomes. Both exogenously added DA–α-syn (Figure 7) and endogenous α-syn in cells with increased cytosolic dopamine (Figure 6) bound with higher affinity to the lysosomal membrane than their unmodified counterparts.

Although there is no reliable method for the detection of DA–α-syn inside cells, we provide in this study independent evidence to support the belief that DA–α-syn is responsible for the inhibitory effect on CMA: (a) this effect is not observed in dopaminergic neuronal cultures lacking α-syn (Figure 5), indicating that cellular presence of α-syn is necessary; (b) this effect is not observed in cells expressing a dopamine-insensitive mutant form of α-syn (Figure 6), indicating that the presence of α-syn is not sufficient but that it has to be susceptible to dopamine modification; (c) this inhibitory effect can be reproduced when DA–α-syn is presented to isolated lysosomes (the most direct approach for measuring CMA, as the effect of other proteolytic systems or cellular factors is eliminated); (d) the inhibition of CMA activity in lysosomes isolated from cells with increased cytosolic levels of dopamine and which have associated with their membrane endogenous α-syn is remarkably similar to that observed in the in vitro system. Furthermore, this effect is only observed in cells expressing α-syn susceptible to dopamine modification.

The dopamine-modified exogenous and endogenous proteins were detected at the lysosomal membrane in oligomeric complexes (Figure 6D and Figure 7, B and C). In contrast to the covalently linked oligomeric forms of nitrated α-syn, oligomers formed from DA–α-syn inhibited CMA. The different consequences of the binding of both oligomeric structures to lysosomes could arise from the sequence of events that led to their association with the membranes: nitrated oligomers bound to the lysosomal membrane as oligomeric structures and, as we observed no competition, apparently to sites different from those of CMA substrates. In contrast, DA–α-syn oligomers appeared to form at the lysosomal membrane after binding as monomers to the CMA translocation complex. These results suggest that membrane-bound DA–α-syn monomers act as nucleation seeds, resulting in the formation of CMA-blocking multimeric complexes at the lysosomal membrane, visualized as slow migrating forms of α-syn by electrophoresis (Figure 6E and Figure 7A) and large-size clusters of gold particles by immunogold (Figure 6D and Figure 7, B and C). Future attempts to prevent the blockage of CMA by DA–α-syn should consider interventions aimed to diminish or revert oligomerization of the modified protein at the lysosomal membrane. Furthermore, in light of the pathogenic effect of the accumulation of α-syn in other neuronal populations and in glia in other synucleinopathies (4), it would be interesting to determine in the future additional cell-type–dependent effects of the posttranslational modifications of α-syn on the autophagic system.

Methods

Animals

Male Wistar rats (200–250 g) fasted for 20 hours before sacrifice were used. Synuclein-null (–/–) mice were generated as described (39). All animal studies were conducted under an animal study protocol approved by the Albert Einstein College of Medicine Animal Institute Animal Care and Use Committee.

Cultured cells

Primary midbrain neuronal cultures. VM neurons and cortical neurons were obtained from day 0–2 postnatal mice expressing GFP under a TH promoter (TH-GFP) that identifies living dopaminergic neurons (43). Cells were dissociated and cultured on monolayers of cortical astrocytes, as previously described (44). Postnatally derived cultures prepared in this fashion contained approximately 40% dopamine neurons. Experiments were conducted 1 to 2 weeks after plating.

SH-SY5Y cells. SH-SY5Y cells (CRL-2266; ATCC) stably expressing wild-type α-syn or the mutant form insensitive to dopamine-induced noncovalent alterations (125-YEMPS-129→125-FAAFA-129; ref. 18) were maintained in DMEM:F12 medium (Invitrogen) supplemented with 10% heat-inactivated fetal bovine serum. For each experiment, cells were transduced with 3×10^6 infectious units/ml of lentivirus containing empty pTY vector or pTY-TH-RR-EE vector (encoding for the RR-EE mutant form of human TH-1, which increases intracellular levels of dopamine), as described before (29). At this MOI, 45%–50% of cells should transduce. All cells were differentiated by treatment with 20 μM retinoic acid for 9 days, then harvested for analysis.

Chemicals, antibodies, and proteins

Sources of reagents were as described previously (9, 10, 27). The antibody against mouse α-syn was from Transduction Laboratories. For Figure 6 and Supplemental Figure 4, the monoclonal antibody Syn204 (39) was used. The antibody against nitrotyrosine was generated as described (27). Synucleins were expressed as recombinant proteins in *E. coli* as described previously (27). The expression construct encoding S/E α-syn was created using standard PCR mutagenesis methodology and was confirmed by DNA sequencing.

Modification of α-syn

Irreversible covalent modifications of wild-type purified α-syn were performed as follows:

Oxidation. Metal-catalyzed oxidation of α-syn was carried out dialyzing α-syn (1 mg protein) against 50 volumes of HEPES buffer (50 mM HEPES, pH 7.2, 100 mM KCl, 10 mM $MgCl_2$) supplemented or not (mock) with 25 mM ascorbic acid and 0.1 mM $FeCl_3$ at 37°C. The oxidative reaction was stopped by adding 1 mM EDTA, and the samples were dialyzed against HEPES buffer for 24 hours with 4 changes. The first 2 changes were sup-

plemented with 1 mM EDTA. The efficiency of oxidation was monitored by comparing levels of the Coomassie blue–stained protein with those detected with the antibody against α-syn or an antibody specific against carbonyl groups after sample derivatization using the Oxidized Protein Detection Kit (OxyBlot) from Chemicon International. The exposure to oxidants was adjusted to result in soluble oxidized monomeric α-syn, since extensive oxidation of α-syn results in the formation of aggregates. Incubation of α-syn with the oxidant mixture for 90 minutes was determined to be sufficient to oxidize the protein but did not induce aggregation.

Phosphorylation. Both in vitro phosphorylation and emulation of phosphorylation by replacing serine 129 of α-syn with the negatively charged residue glutamic acid (S129E) were used in this study. This amino acid replacement has been shown to mimic the biochemical, biophysical, and toxic properties of the phosphorylation described for α-syn in brain tissues from PD patients (16). Amino acid replacement proved to be a better method than in vitro phosphorylation, as it guaranteed that the protein remained phosphorylated after exposure to the lysosomal fraction, which is highly enriched in phosphatases: we found high variability among samples when we used an in vitro phosphorylated form of the protein (data not shown), attributable to partial dephosphorylation of the protein during the incubation. Consequently, only the phosphorylation-like mutant was used for quantitative analysis.

Nitration. α-Syn (10 mg/ml) was diluted into 200 mM potassium phosphate, pH 7.0, 25 mM $NaHCO_3$, and 0.1 mM diethylenetriaminepentaacetic acid. Peroxynitrite was added to produce a final 5-molar excess of the protein concentration as previously described (27). The different nitrated α-syn species, monomeric, dimeric, and oligomeric, were separated by gel filtration through a Superdex 200 matrix (Amersham).

Reaction with dopamine. α-Syn (14 μM) was incubated in Dulbecco's phosphate buffer, pH 7.4, in the presence of dopamine or its oxidized product dopaminochrome. A 1:1 stoichiometry was selected because exposure to dopamine under these conditions rendered only monomers of α-syn with no detectable formation of oligomers after 3 hours of incubation. A mutant form of α-syn insensitive to the dopamine-induced noncovalent conformational alterations (18) was used as control where indicated. In this protein, the residues $Y_{125}EMPS_{129}$ had been replaced by $F_{125}AAFA_{129}$.

None of these modifications interfered with the ability of the antibody against α-syn to recognize these proteins, as determined by comparing Coomassie blue staining and immunoblot of the purified proteins subjected to SDS-PAGE (data not shown). It is also unlikely that the ability of the antibody to detect the modified forms changed once they were translocated into lysosomes, since incubation of the modified forms of α-syn with lysosomal matrices in the presence of protease inhibitors did not affect their recognition by the antibody (data not shown) and no other molecular weight forms of the protein were detected in the immunoblot.

Isolation of lysosomes

Rat liver lysosomes were isolated from a light mitochondrial-lysosomal fraction in a discontinuous metrizamide density gradient by the shorter method described previously (23). Lysosomal integrity was verified after isolation by measuring the activity of β-hexosaminidase, a lysosomal enzyme, in the incubation medium (38). Preparations with more than 10% broken lysosomes immediately after isolation or more than 20% at the end of the incubation were discarded. A lysosomal-enriched fraction was isolated from cultured cells by differential centrifugation as described previously (38).

Uptake of substrate proteins by isolated lysosomes

Transport of purified proteins into isolated lysosomes was analyzed using a previously described in vitro system (23, 24, 45). In brief, wild-type α-syn, modified α-syn, or GAPDH was incubated with freshly isolated rat liver lysosomes in 3-(*N*-morpholino) propanesulfonic acid (MOPS) buffer (10 mM MOPS, pH 7.3, 0.3 M sucrose) for 20 minutes at 37°C. Where indicated, lysosomes were preincubated with a cocktail of proteinase inhibitors for 10 minutes at 0°C (23). Lysosomes were collected by centrifugation, washed with MOPS buffer, and subjected to SDS-PAGE and immunoblotting with antibodies specific for the assayed protein. Uptake was calculated by subtracting the protein associated with lysosomes in the presence (protein bound to the lysosomal membrane and taken up by lysosomes) and absence (protein bound to the lysosomal membrane) of inhibitors of lysosomal proteases, as described (9, 25). In the absence of protease inhibitors, the substrate that reaches the lysosomal lumen is rapidly degraded and the only substrate remaining is that bound to the lysosomal membrane. If lysosomal proteases are blocked, both the membrane-bound protein and that translocated into the lumen can be detected. Uptake is calculated as the difference between the amount of substrate associated with protease inhibitor–treated lysosomes and that bound to the lysosomal membrane without protease inhibitors.

Degradation of proteins by isolated lysosomes

Lysosomal degradation of exogenously added proteins was assayed as described before (24) by incubation in MOPS buffer supplemented with 1 mM DTT and 5.6 μM cysteine of intact lysosomes with GAPDH radiolabeled by reductive methylation ([^{14}C]GAPDH; 1.2×10^6 dpm/nmol) (23). Reactions were stopped with a final concentration of 10% trichloroacetic acid, and after filtration in the Millipore Multiscreen Assay System (Millipore) with a 0.22-μm pore membrane, radioactivity in the flow-through was measured in a WinSpectral 1414 liquid scintillation counter (PerkinElmer). Proteolysis was expressed as the percentage of the initial acid-precipitable radioactivity (protein) transformed to acid-soluble radioactivity (amino acids and small peptides) during the incubation time.

Intracellular protein degradation

Total protein degradation in cultured cells was measured by pulse-chase experiments (9). Confluent cells were labeled with [^{3}H]leucine (2 μCi/ml) (NEN; PerkinElmer) for 48 hours at 37°C and then extensively washed and maintained in complete or serum-deprived medium with an excess of unlabeled leucine. Aliquots of the medium taken at different times were precipitated in trichloroacetic acid and proteolysis measured as above. Total radioactivity incorporated in cellular proteins was determined in triplicate samples as the amount of acid-precipitable radioactivity in labeled cells immediately after washing. Proteolysis was calculated as the percentage of acid-precipitable radioactivity (protein) transformed in acid-soluble radioactivity (amino acids and peptides) at the different analyzed times. Values were expressed as percentages of protein degraded per hour considering the linear slope of the logarithmic plotting (25, 46, 47). Where indicated, 15 mM ammonium chloride and 100 μM leupeptine or 10 mM 3-methyladenine was added in the culture medium during the chase. The former combination effectively blocks all types of autophagy, as it reduces the activity of all lysosomal proteases by increasing the lumenal lysosomal pH without affecting the activity of other intracellular proteolytic systems (25). Blockage of macroautophagy was attained with the PI3K inhibitor 3-methyladenine, previously shown not to modify CMA activity in cultured cells (13, 46). The inhibitory effect of the different proteins and treatments on the lysosomal system was calculated as the decrease in protein degradation sensitive to ammonium chloride, while the inhibitory effect on macroautophagy was determined as the decrease in protein degradation sensitive to ammonium chloride that is also inhibited by 3-methyladenine. Finally, CMA-dependent degradation was calculated as the percentage of protein degradation sensi-

tive to ammonium chloride that is not inhibited by 3-methyladenine, and the inhibitory effect of the proteins and treatments analyzed in this work on CMA activity were determined as changes in this percentage. The combination of these inhibitors used to assess the contribution of the different forms of autophagy to intracellular protein degradation has been extensively reported on before (13, 25, 46, 47).

Intracellular patch electrochemistry

Measurements of cytosolic dopamine concentrations in VM neurons from TH-GFP mice were performed as previously described (32). In brief, a polyethylene-coated 5-μm carbon fiber electrode was placed inside the glass patch pipette and used in a cyclic voltammetric mode of detection (scan rate of 250 mV/ms) using a subroutine locally written in Igor Pro (WaveMetrics Inc.). After achieving a seal between the cell and the patch pipette, the plasma membrane was ruptured by suction, and substances diffusing from the cytosol into the pipette were observed as a slow wave of oxidation current. The cultures were incubated with 100 μM L-DOPA for 1 hour prior to and during the recordings. After background current subtraction, dopamine concentration at the pipette tip was calculated using calibration curves generated for carbon fiber electrodes with different exposed surfaces (34). The initial concentration of cytosolic dopamine was calculated using the neuronal cell body volume and the volume of the pipette tip estimated from photographs acquired before each recording. As the volume of the organelles that occupy neuronal cytosol is unknown, cytosolic dopamine concentrations estimated from intracellular patch electrochemistry recordings were most likely underestimated.

Total cellular levels of catechol were quantified by high-performance liquid chromatography with an electrochemical detection method by comparing to known amount of standards as described before (20, 34, 36).

Lentiviral-mediated RNAi in VM neuron cultures

RNAi against LAMP-2A was performed using the shRNAi against the 5′-CTGCAATCTGATTGATTA-3′ sequence of the 1331–1359 bases in exon 8A of the *Lamp-2* gene. The hairpin of this sequence along with the H1 promoter was subcloned from the pSuper vector (described in ref. 13) into the pCCL.PPT.hPGK.GFP.Wpre vector (48). Vesicular stomatitis virus–pseudotyped lentiviral stocks were prepared by transient cotransfection of the shRNAi-carrying vector or empty vector along with the third-generation packaging constructs pMDLg/pRRE, pRSV-REV, and the pMD2.G envelope into 293T cells, as described (48). For transduction, VM-cultured neurons were incubated with 1×10^7 transducing units of concentrated lentivirus at 37°C for 24 hours. After a 1:1 dilution, cells were incubated for another 48 hours and then changed to virus-free fresh medium. The efficiency of RNAi was verified by real-time PCR, immunoblot, and immunofluorescence with an antibody against LAMP-2A at different times. Due to the long half-life of the LAMP-2A protein, we estimated that an 80% decrease in intracellular levels of the protein would not be attained until 5 days after infection. Consequently, the different treatments were all applied after that day. VM cultures infected with the shRNAi or the empty carrying vector were incubated with 100 μM L-DOPA for 48 hours, and the number of neurons remaining after each treatment was calculated after fixation using an Axiovert 200 (Zeiss) fluorescence microscope as described before (30). At least 10 randomly chosen observation fields for each sample were counted from 2 independent samples of each condition.

Electron microscopy and immunogold

Immunogold labeling was performed as described previously (23) using an antibody against α-syn for 12 hours, followed by gold secondary (GAR 1:100) for 2 hours. Samples were water rinsed and negatively stained with 1% uranyl acetate. Appropriate controls using only the gold-conjugated secondary antibodies were included. All grids were viewed on a JEOL 100CX II transmission electron microscope at 80 kV.

General methods

Protein concentration was determined by the Lowry method using bovine serum albumin as a standard. Lysosomal enzymatic activities were measured as reported (38). After SDS-PAGE and immunoblotting, the proteins recognized by the specific antibodies were visualized by chemiluminescence methods (Renaissance; NEN-Life Science Products) as described previously (9). Membranes were exposed to BioMax Light Kodak films (Kodak Scientific Films) for increasing periods of time ranging from 5 seconds to 10 minutes. Densitometric quantification of the immunoblotted membranes was performed with an Image Analyzer System (Inotech S-100). For each of the forms of synuclein used in this study, we prepared standard densitometric curves (intensity vs. μg of protein) from 3 immunoblots containing increasing concentrations of the purified protein (0.2 μg to 20 μg). The intensity of the bands was quantified using the square "spot denso" routine of the Image Analyzer System. For each protein band, the intensity value obtained from empty squares of the same size to the protein bands drawn above each of them was discounted as background. The amount of α-syn in the experiments was adjusted to obtain intensity values inside the linear range in the standard curves. From the different exposures of each membrane, we chose those in which no bands were saturated. In addition, each gel contained 1 or 2 lanes with a known amount of the purified proteins to provide normalization of the densitometric values from experiment to experiment. Two-tailed Student's *t* test for unpaired data was used for statistical analysis.

Acknowledgments

We are grateful to Frank Macaluso and Leslie Gunther (Analytical Imaging Facility at the Albert Einstein College of Medicine) for their valuable assistance with electron microscopy and immunogold procedures and to Roberta Kiffin for assistance in the preparation of this manuscript. This work was supported by National Institute of Neurological Disorders and Stroke Udall Center grants (to D. Sulzer, S. Przedborski, and P. Lansbury), NIH/National Institute of Aging grants (AG021904 and AG19834 to A.M. Cuervo; AG13966 to H. Ischiropoulos), the Picower Foundation (to D. Sulzer), the Parkinson's Disease and Lowenstein Foundations (to D. Sulzer and W. Dauer), and an Ellison Medical Foundation Award (to A.M. Cuervo). A.C. Massey is supported by NIH/NIA training grant T32AG023475.

Received for publication May 25, 2007, and accepted in revised form October 22, 2007.

Address correspondence to: Ana Maria Cuervo, Department of Anatomy and Structural Biology, Albert Einstein College of Medicine, Ullmann Building, Room 611, 1300 Morris Park Avenue, New York, New York 10461, USA. Phone: (718) 430-2689; Fax: (718) 430-8975; E-mail: amcuervo@aecom.yu.edu.

1. Volles, M., and Lansbury, P.J. 2003. Zeroing in on the pathogenic form of alpha-synuclein and its mechanism of neurotoxicity in Parkinson's disease. *Biochemistry.* **42**:7871–7878.
2. Abeliovich, A., et al. 2000. Mice lacking alpha-synuclein display functional deficits in the nigrostriatal dopamine system. *Neuron.* **25**:239–252.
3. Nussbaum, R.L., and Polymeropoulos, M.H. 1997. Genetics of Parkinson's disease. *Hum. Mol. Genet.* **6**:1687–1691.
4. Lee, V.M, and Trojanowski, J.Q. 2006. Mechanisms of Parkinson's disease linked to pathological alpha-synuclein: new targets for drug discovery. *Neuron.* **52**:33–38.
5. Wilson, C., et al. 2004. Degradative organelles con-

taining mislocalized {alpha}- and {beta}-synuclein proliferate in presenilin-1 null neurons. *J. Cell Biol.* **165**:335–346.
6. Webb, J., Ravikumar, B., Atkins, J., Skepper, J., and Rubinsztein, D. 2003. Alpha-Synuclein is degraded by both autophagy and the proteasome. *J. Biol. Chem.* **278**:25009–25013.
7. Stefanis, L., Larsen, K.E., Rideout, H.J., Sulzer, D., and Greene, L.A. 2001. Expression of A53T mutant but not wild-type alpha-synuclein in PC12 cells induces alterations of the ubiquitin-dependent degradation system, loss of dopamine release, and autophagic cell death. *J. Neurosci.* **21**:9549–9560.
8. Tanaka, Y., et al. 2001. Inducible expression of mutant alpha-synuclein decreases proteasome activity and increases sensitivity to mitochondria-dependent apoptosis. *Hum. Mol. Genet.* **10**:919–926.
9. Cuervo, A.M., Stefanis, L., Fredenburg, R., Lansbury, P.T., and Sulzer, D. 2004. Impaired degradation of mutant alpha-synuclein by chaperone-mediated autophagy. *Science.* **305**:1292–1295.
10. Cuervo, A.M., and Dice, J.F. 1996. A receptor for the selective uptake and degradation of proteins by lysosomes. *Science.* **273**:501–503.
11. Majeski, A., and Dice, J. 2004. Mechanisms of chaperone-mediated autophagy. *Int. J. Biochem. Cell Biol.* **36**:2435–2444.
12. Klionsky, D.J. 2005. Autophagy. *Curr. Biol.* **15**:R282–R283.
13. Massey, A.C., Kaushik, S., Sovak, G., Kiffin, R., and Cuervo, A.M. 2006. Consequences of the selective blockage of chaperone-mediated autophagy. *Proc. Natl. Acad. Sci. U. S. A.* **103**:5805–5810.
14. Iwata, A., et al. 2005. Increased susceptibility of cytoplasmic over nuclear polyglutamine aggregates to autophagic degradation. *Proc. Natl. Acad. Sci. U. S. A.* **102**:13135–13140.
15. Paxinou, E., et al. 2001. Induction of alpha-synuclein aggregation by intracellular nitrative insult. *J. Neurosci.* **21**:8053–8061.
16. Smith, W., et al. 2005. Alpha-synuclein phosphorylation enhances eosinophilic cytoplasmic inclusion formation in SH-SY5Y cells. *J. Neurosci.* **25**:5544–5552.
17. McFarlane, D., Dybdal, N., Donaldson, M., Miller, L., and Cribb, A. 2005. Nitration and increased alpha-synuclein expression associated with dopaminergic neurodegeneration in equine pituitary pars intermedia dysfunction. *J. Neuroendocrinol.* **17**:73–80.
18. Norris, E., et al. 2005. Reversible inhibition of alpha-synuclein fibrillization by dopaminochrome-mediated conformational alterations. *J. Biol. Chem.* **280**:21212–21219.
19. Maguire-Zeiss, K., Short, D., and Federoff, H. 2005. Synuclein, dopamine and oxidative stress: co-conspirators in Parkinson's disease? *Brain Res. Mol. Brain. Res.* **134**:18–23.
20. Burke, W.J., Li, S.W., Williams, E.A., Nonneman, R., and Zahm, D.S. 2003. 3,4-Dihydroxyphenylacetaldehyde is the toxic dopamine metabolite in vivo: implications for Parkinson's disease pathogenesis. *Brain Res.* **989**:205–213.
21. Conway, K., Rochet, J., Bieganski, R., and Lansbury PT, J. 2001. Kinetic stabilization of the alpha-synuclein protofibril by a dopamine-alpha-synuclein adduct. *Science.* **294**:1346–1359.
22. Aniento, F., Roche, E., Cuervo, A.M., and Knecht, E. 1993. Uptake and degradation of glyceraldehyde-3-phosphate dehydrogenase by rat liver lysosomes. *J. Biol. Chem.* **268**:10463–10470.
23. Cuervo, A.M., Dice, J.F., and Knecht, E. 1997. A lysosomal population responsible for the hsc73-mediated degradation of cytosolic proteins in lysosomes. *J. Biol. Chem.* **272**:5606–5615.
24. Terlecky, S.R., and Dice, J.F. 1993. Polypeptide import and degradation by isolated lysosomes. *J. Biol. Chem.* **268**:23490–23495.
25. Salvador, N., Aguado, C., Horst, M., and Knecht, E. 2000. Import of a cytosolic protein into lysosomes by chaperone-mediated autophagy depends on its folding state. *J. Biol. Chem.* **275**:27447–27456.
26. Volles, M.J., et al. 2001. Vesicle permeabilization by protofibrillar alpha-synuclein: implications for the pathogenesis and treatment of Parkinson's disease. *Biochemistry.* **40**:7812–7819.
27. Hodara, R., et al. 2004. Functional consequences of a-synuclein tyrosine nitration: diminished binding to lipid vesicles and increased fibril formation. *J. Biol. Chem.* **279**:47746–47753.
28. Caughey, B., and Lansbury, P.T. 2003. Protofibrils, pores, fibrils, and neurodegeneration: separating the responsible protein aggregates from the innocent bystanders. *Annu. Rev. Neurosci.* **26**:267–298.
29. Larsen, K., Fon, E., Hastings, T., Edwards, R., and Sulzer, D. 2002. Methamphetamine-induced degeneration of dopaminergic neurons involves autophagy and upregulation of dopamine synthesis. *J. Neurosci.* **22**:8951–8960.
30. Pothos, E.N., Desmond, M., and Sulzer, D. 1996. L-3,4-Dihydroxyphenylalanine increases the quantal size of exocytic dopamine release in vitro. *J. Neurochem.* **66**:629–636.
31. Mosharov, E., et al. 2006. Alpha-synuclein overexpression increases cytosolic catecholamine concentration. *J. Neurosci.* **26**:9304–9311.
32. Mosharov, E., Gong, L., Khanna, B., Sulzer, D., and Lindau, M. 2003. Intracellular patch electrochemistry: regulation of cytosolic catecholamines in chromaffin cells. *J. Neurosci.* **23**:5835–5845.
33. Sulzer, D., et al. 2000. Neuromelanin biosynthesis is driven by excess cytosolic catecholamines not accumulated by synaptic vesicles. *Proc. Natl. Acad. Sci. U. S. A.* **97**:11869–11874.
34. Mena, M., et al. 1997. Effects of wild-type and mutated copper/zinc superoxide dismutase n neuronal survial and L-DOPA induced toxicity in postnatal midbrain culture. *J. Neurochem.* **69**:21–33.
35. Dauer, W., et al. 2002. Resistance of alpha-synuclein null mice to the Parkinsonian neurotoxin MPTP. *Proc. Natl. Acad. Sci. U. S. A.* **99**:14524–14529.
36. Mazzulli, J., et al. 2006. Cytosolic catechols inhibit alpha-synuclein aggregation and facilitate the formation of intracellular soluble oligomeric intermediates. *J. Neurosci.* **26**:10068–10078.
37. Cuervo, A.M., and Dice, J.F. 2000. Unique properties of lamp2a compared to other lamp2 isoforms. *J. Cell Sci.* **113**:4441–4450.
38. Storrie, B., and Madden, E.A. 1990. Isolation of subcellular organelles. *Meth. Enzymol.* **182**:203–225.
39. Giasson, B.I., et al. 2000. A panel of epitope-specific antibodies detects protein domains distributed throughout human alpha-synuclein in Lewy bodies of Parkinson's disease. *J. Neurosci. Res.* **59**:528–533.
40. Kiffin, R., Christian, C., Knecht, E., and Cuervo, A.M. 2004. Activation of chaperone-mediated autophagy during oxidative stress. *Mol. Biol. Cell.* **15**:4829–4840.
41. Payton, J., Perrin, R., Woods, W., and George, J. 2004. Structural determinants of PLD2 inhibition by alpha-synuclein. *J. Mol. Biol.* **337**:1001–1009.
42. Cappai, R., et al. 2005. Dopamine promotes alpha-synuclein aggregation into SDS-resistant soluble oligomers via a distinct folding pathway. *FASEB J.* **19**:1377–1379.
43. Sawamoto, K., et al. 2001. Visualization, direct isolation, and transplantation of midbrain dopaminergic neurons. *Proc. Natl. Acad. Sci.* **98**:6423–6428.
44. Pothos, E.N., et al. 2000. Synaptic vesicle transporter expression regulates vesicle phenotype and quantal size. *J. Neurosci.* **20**:7297–7306.
45. Cuervo, A.M. 2004. Autophagy: in sickness and in health. *Trends Cell Biol.* **14**:70–77.
46. Finn, P., Mesires, N., Vine, M., and Dice, J.F. 2005. Effects of small molecules on chaperone-mediated autophagy. *Autophagy.* **1**:141–145.
47. Klionsky, D., Cuervo, A., and Seglen, P. 2007. Methods for monitoring autophagy from yeast to human. *Autophagy.* **3**:181–206.
48. Follenzi, A., and Naldini, L. 2002. HIV-based vectors. Preparation and use. *Methods Mol. Med.* **69**:259–274.